taining two time steps are obtained. Excellent expositions on this rule are found in Refs. 5–7.

III. Results and Discussion

The numerical results presented in this section were obtained using a computer code written in *Mathematica*. It should be remarked that using a hybrid method that links the *Mathematica* code (used for setting up the matrix equations) to either a C or Fortran code (used for performing the iteration operations), would produce a highly effective computational procedure.

In the tables presented here, the underlined results correspond to actual collocation positions where the residual is forced to be zero.[1] For the sake of comparison with Frankel,[1] Table 1 presents results for the reconstructed physical variables of dimensionless temperature $\theta_N(\eta, \xi)$ and dimensionless radiative heat flux $Q_N^r(\eta, \xi)$ as both a function of the time step $\Delta\xi$ used in solving the expansion coefficients, and the order of the approximation N when the conduction/radiation number is $N_{cr} = 0.1$, the single-scattering albedo is $\omega = 0.5$, the dimensionless half width is $\alpha = 0.5$, and the dimensionless initial temperature and defined surface temperature at $\eta = 1$ are $\theta_i = \theta_2 = 0$, respectively. The results indicated in Table 1 correspond well with those of the explicitly obtained results reported by Frankel,[1] which in turn support the results described by other investigators.

In most reported studies, sparse numerical accounts have been documented for the extremal values of the single-scattering albedo, i.e., $\omega = 0, 1$. It should be noted that the numerical results presented in Table 2 were obtained without any modification to the general computer code developed for $\omega\varepsilon(0, 1)$. Table 2a presents numerical results for both the dimensionless temperature $\theta_N(\eta, \xi)$ and dimensionless radiative heat flux $Q_N^r(\eta, \xi)$ as both a function of the time step $\Delta\xi$ used in solving the expansion coefficients and the order of the approximation N when $N_{cr} = 0.1$, $\omega = 0$, $\alpha = 0.5$, and $\theta_i = \theta_2 = 0$. By comparing the results of Table 2a to the results of Table 1, it is clear that additional energy is available for absorption when the single-scattering albedo is decreased. This corresponds to an increase in the temperature distribution as indicated in Table 2a.

Table 2b presents tabulated dimensionless temperature and radiative heat flux results for the conservative case ($\omega = 1$) when $N_{cr} = 0.1$, $\alpha = 0.5$, and $\theta_i = \theta_2 = 0$ for various time step sizes $\Delta\xi$ and various orders of the approximation N. It is well-known that under this situation the radiative heat flux is constant as clearly seen in this table. Also, the resulting temperature distribution is in line with physical expectations in comparison with Tables 1 and 2a.

The mathematical formalism described by Frankel[1] and computationally refined here offers an alternative methodology for solving transient mixed-mode transport. Additional studies are underway generalizing the methodology to multidimensional geometries and various degrees of anisotropy.

Acknowledgment

This work was supported under Grant CCR-9320385 provided by the National Science Foundation.

References

[1]Frankel, J. I., "Cumulative Variable Formulation for Transient Conductive and Radiative Transport in Participating Media," *Journal of Thermophysics and Heat Transfer*, Vol. 9, No. 2, 1995, pp. 210–218.

[2]Frankel, J. I., "A New Orthogonal Collocation Integral Formulation to Transient Radiative Transport," *Boundary Element Technology IX*, Computational Mechanics Publication, Southampton, England, UK, 1994, pp. 51–58.

[3]Frankel, J. I., and Choudhury, S. R., "Some New Observations on the Classical Logistic Equation with Heredity," *Applied Mathematics and Computation*, Vol. 58, 1993, p. 275–308.

[4]Kumar, S., and Sloan, I. H., "A New Collocation-Type Method for Hammerstein Integral Equations," *Mathematics of Computation*, Vol. 48, No. 178, 1987, pp. 585–593.

[5]Linz, P., "Analytical and Numerical Methods for Volterra Equations," Society for Industrial and Applied Mathematics, Philadelphia, PA, 1985.

[6]Baker, C. T. H., *The Numerical Treatment of Integral Equations*, Clarendon, Oxford, England, UK, 1978.

[7]Delves, L. M., and Mohamad, J. L., *Computational Methods for Integral Equations*, Cambridge Univ. Press, Cambridge, England, UK, 1988.

[8]Wolfram, S., *Mathematica: A System for Doing Mathematics by Computer*, 2nd ed., Addison-Wesley, New York, 1991.

Towards a Theory of the Surface Conductance Coefficient in Solids

María L. Cancillo* and Juan J. Morales†
Universidad de Extremadura, Badajoz, Spain 06071

Nomenclature

c	=	specific heat
H	=	surface conductance coefficient
K	=	thermal conductivity
p	=	perimeter
sqdif	=	sum of the squares of the differences between the experimental data T_{ie} and the theoretical values T_{it}
T	=	temperature
T_0	=	constant temperature of the medium
t	=	time
w	=	cross section
x	=	coordinate in the axial direction
ρ	=	density

Introduction

THE surface conductance coefficient appears in a term of the differential equation for heat flow, which for the one-dimensional case takes the form:

$$\frac{\partial T}{\partial t} = \frac{K}{\rho c}\frac{\partial^2 T}{\partial x^2} - \frac{Hp}{\rho c w}(T - T_0) \tag{1}$$

Table 1 Parameters for the fit of the experimental steady-state data to the single exponential law of Eq. (2)

Cases	$T_1 \pm \sigma$	$-m \pm \sigma$	H, Eq. (3)	*sqdif*
I	75.2 ± 0.6	0.99 ± 0.05	2.35	17.37
II	68.1 ± 0.6	1.01 ± 0.05	2.44	15.12
III	65.0 ± 0.6	1.00 ± 0.06	2.39	13.13
IV	56.0 ± 0.5	0.97 ± 0.03	2.25	9.45
V	49.7 ± 0.4	0.97 ± 0.03	2.25	7.34
VI	43.0 ± 0.4	0.93 ± 0.03	2.07	5.18
VII	39.7 ± 0.4	0.88 ± 0.03	1.85	2.98
VIII	33.8 ± 0.4	0.92 ± 0.03	2.03	3.14
IX	30.2 ± 0.4	0.87 ± 0.03	1.81	1.63
X	23.5 ± 0.4	0.89 ± 0.04	1.90	1.47
XI	20.1 ± 0.4	0.82 ± 0.04	1.61	0.63
XII	13.9 ± 0.4	0.85 ± 0.04	1.65	0.33
Means	$\bar{m} = 0.92 \pm 0.06$		$\bar{H} = 2.03 \pm 0.12$	

Received Dec. 20, 1993; revision received Feb. 25, 1994; accepted for publication Feb. 25, 1994.

*Associated Lecturer, Department of Physics, Faculty of Sciences.
†Lecturer, Department of Physics, Faculty of Sciences.

Table 2 Values of the fit of the experimental data to the single exponential law of Eq. (2), for the cooling of the first point of the bar

Cases	Cooling time, s	ΔT, °C	$T_{i=1} \pm \sigma$	$-(m' \pm \sigma) \times 10^{-3}$	H, Eq. (3)	*sqdif*
I	12,000	1.4	80.2 ± 0.9	0.369 ± 0.005	7.97	12.56
II	9,900	1.7	69.2 ± 0.9	0.415 ± 0.007	8.96	17.98
III	9,900	1.7	66.3 ± 0.9	0.412 ± 0.008	8.90	16.79
IV	9,900	1.6	56.3 ± 0.9	0.400 ± 0.009	8.64	13.47
V	9,900	1.4	50.3 ± 0.9	0.40 ± 0.01	8.64	9.13
VI	9,900	1.7	46.1 ± 0.9	0.354 ± 0.009	7.65	2.61
VII	9,900	1.4	44.2 ± 0.9	0.360 ± 0.009	7.78	2.33
VIII	9,900	1.3	34.2 ± 0.9	0.39 ± 0.01	8.43	3.02
IX	9,900	1.4	32.8 ± 0.9	0.34 ± 0.01	7.35	2.93
X	8,400	1.3	24.4 ± 0.9	0.38 ± 0.02	8.21	1.79
XI	7,800	1.4	22.1 ± 0.9	0.35 ± 0.02	7.56	0.10
XII	6,300	1.3	14.0 ± 0.9	0.39 ± 0.04	8.42	0.25
Means		$\bar{m}' = 0.38 \pm 0.02$			$\bar{H} = 8.2 \pm 0.4$	

In principle,[1,2] H can be obtained from Eq. (1) either from the steady state $(\partial T/\partial t) = 0$, or from cooling $(\partial^2 T/\partial x^2) = 0$, both of whose solutions obey a single exponential law given, respectively, by

$$T_i = T_1 \exp(-mx) \quad \text{and} \quad T' = T_i \exp(-m't) \qquad (2)$$

where

$$m^2 = Hp/Kw \quad \text{and} \quad m' = Hp/\rho cw \qquad (3)$$

Experimentally, therefore, the idea was to look at steady-state and cooling temperature distributions in the same bar of a given material to see whether these exponential distributions were satisfied and yielded the same value for H.

We used a standard cylindrical copper[3] bar 42 cm long, and 2.5 cm in diameter. The bar was insulated by wrapping it with asbestos cord and it was held in place on two wooden supports in the lab at a constant air temperature, with only one exposed face. J-type thermocouples (Fe-Constantan, from −200°C to +800°C) were placed in 10 holes drilled perpendicularly into the bar along its length, with its temperatures being recorded automatically using a data-logger (Fluke, Helios model). The first thermocouple was 7 cm from the end, being electrically heated by a resistive coil, and the others were 3.6, 7.1, 10.6, 14.0, 17.5, 20.9, 24.4, 27.9, and 31.4 cm from the first. The thermocouples were previously calibrated to ensure that the maximum difference between them was less than the individual accuracy of ±0.1°C.

An identical setup had been used for iron, aluminium, and polymethyl methacrylate bars,[4-6] and as described there, 12 steady-state cases were studied, with a temperature range from 14 to 75°C excess over room temperature as measured for the first (hottest) point. For each of the 12 cases, the cooling of each of the 10 points was measured. The first (hottest) point will be analyzed here as being the worst adjusted to the simple theory, but the other points do not change the qualitative conclusions in any way.

Table 1 lists the results of fitting the steady-state experimental data to a single exponential law as in Eq. (2). The mean values of m and H are $\bar{m} = 0.92 \pm 0.06$, and $\bar{H} = 2.03 \pm 0.12$. The goodness of the fit, however, becomes worse very fast as one approaches the hotter regimes, as can be seen in the last column: the *sqdif* values in cases I–VI are too large to consider H as obeying a single exponential, this only being an acceptable assumption for the last few cases IX–XII.

Once the steady states were reached, the cooling was studied. Data were logged every 300 s until the temperature had dropped to 1.3–1.7°C over the surroundings. Table 2 lists the results of the fit to the single exponential law of Eq. (2). The behavior of m' seems to be a constant fluctuating around a mean value $\bar{m}' = 0.38 \pm 0.02$, and hence, from Eq. (3), $\bar{H} = 8.2 \pm 0.4$. A single exponential is an acceptable description of the cooling. Statistically, the value for *sqdif* is better than for the steady state, because there are now two (case XII), three (cases II–XI), and four (case I) times more experimental data than for the steady state. Physically, it is well-known[7] that there exists thermal inertia that can be regarded as a transitory state before entering the cooling regime proper. The values in Table 2 were obtained without eliminating any data. However, the *sqdif* value is reduced 2–3 times (cases I–V) when the first two data points are discarded, the coefficients $T_{i=1}$ are of course lower, and the exponent m' has less dispersion. The rest of the cases (VI–XII) are not affected appreciably.

The steady-state value of H is a factor of 4 smaller than the cooling value (Tables 1 and 2). Comparative results for the other three materials were 1) excellent agreement for iron[4] (15.21 ± 2.34 steady state, vs 15.98 ± 2.36), 2) fair for aluminium[5] (11.9 ± 1.0 vs 8.6 ± 0.4), and 3) poor for polymethyl methacrylate[6] (2.84 ± 0.48 vs 12.8 ± 2.0).

The results obtained in this study show that there is a difficult road ahead towards developing a general theory for the surface conductance coefficient in solids because of this lack of uniformity of the conclusions drawn for different materials under the same experimental conditions, even though these conditions are not too far from Newton's ideal experimental conditions for which Eq. (1) for the heat flow in the bar is supposed to be satisfied. It will be necessary to study a wider range of materials, both good conductors and bad, changing the "ideal" conditions step-by-step over a wider range of temperatures to obtain an algorithm simulating the behavior of a solid under specific thermodynamic conditions, as, e.g., has been done for the estimation of the unsteady heat transfer coefficient.[8]

References

[1]Carslaw, H. S., and Jaeger, J. C., *Conduction of Heat in Solids*, Oxford Univ. Press, Oxford, England, UK, 1978.

[2]Eckert, E. R. G., and Drake, R. M., *Analysis of Heat and Mass Transfer*, McGraw-Hill, Tokyo, 1972.

[3]*Handbook of Chemistry and Physics*, 56th ed., edited by R. C. Weast, CRC Press, Cleveland, OH, 1975–76.

[4]Morales, J. J., "Study of the Surface Conductance Coefficient in a Metallic Bar," *Thermochimica Acta*, Vol. 185, 1991, pp. 255–262.

[5]Morales, J. J., "Towards a Theory of the Surface Conductance Coefficient in Solids. Part 1," *Thermochimica Acta*, Vol. 219, 1993, pp. 343–353.

[6]Morales, J. J., "Study of the Surface Conductance Coefficient in a Plastic Bar," *Thermochimica Acta*, Vol. 194, 1992, pp. 231–237.

[7]Isachenco, V., Osipova, V., and Sukomel, A., *Transmision del Calor*, Marcombo, Barcelona, Spain, 1973.

[8]Hodge, J. K., Chen, A. J., and Hayes, J. R., "Unsteady Heat Transfer Coefficient Estimation for Long Duration," *Journal of Thermophysics and Heat Transfer*, Vol. 2, No. 3, 1988, pp. 218–226.

Thermodynamic Analysis of the Influence of Electric Fields on Frost Formation

H. B. Ma* and G. P. Peterson†
Texas A&M University,
College Station, Texas 77843-3123

Nomenclature

A = surface area
a = height of the needle frost
b = radius of the needle frost
E = average electric field
E_c = electric field at the tip
F = Helmholtz free energy
f = driving force of sublimation
G = Gibbs free energy
g = specific Gibbs free energy
K_{ec} = electric field coefficient
m = mass
p = saturation pressure
p^* = pressure of water vapor near the frost surface
R = universal gas constant
r_c = critical radius of ice nucleation
T = temperature or saturation temperature
γ = interfacial energy of unit area defined by Eq. (9)
ε_0 = dielectric constant
λ = latent heat
ρ = density
χ = polarization rate
ω = specific electric energy

Subscripts
α = solid phase
β = vapor phase
σ = interface phase
0 = relative or reference point
∞ = no electric field

Introduction

THE typical frost formation process in the absence of electrostatic fields has been described in detail by Hayashi et al.[1] In the initial stage of frost formation on a horizontal surface, a thin frost is formed, covering the cooled surface. Frost crystals, which are relatively far apart, then form on this thin frost layer. These frost crystals grow in a vertical direction, all at approximately the same rate, forming a structure of long thin vertical shafts, similar to a forest of trees. This rough frost formation continues to grow through the formation of branches around the top of the frost crystals or through the interaction of each crystal, and gradually forms a relatively flat surface as shown in Fig. 1a.

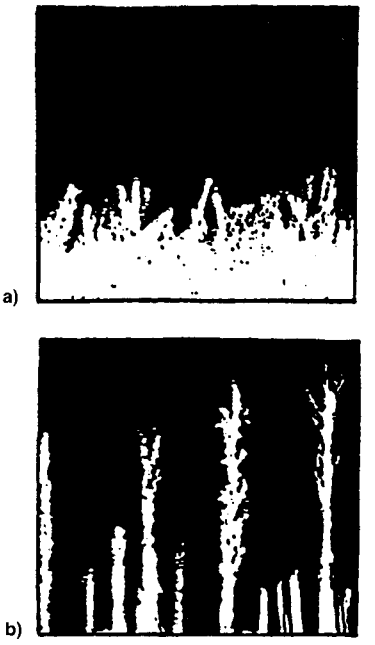

Fig. 1 Schematic of frost formation: a) with and b) without electrostatic fields.

The formation of frost in a uniform electrostatic field is quite different in several respects.[2,3] Most notable is that in the initial frost nucleation, the frost does not appear to form evenly on the cooled surface, but rather forms in pits or small depressions. When the first frost nucleations spread and increase in size, more new frost nucleations are formed on the surface. After a short period of time, small needle-like crystals of frost suddenly appear at the frost nucleation sites. The rate of growth of these needles is quite rapid and not particularly uniform, however, the growth for all of these needles is in the vertical direction, perpendicular to the cooled surface, as shown in Fig. 1b. This behavior has a number of similarities to the formation of liquid droplets occurring in dropwise condensation.

Because little is known about the behavior of these frost needles, and the physical processes involved in the frost growth in the presence of electrostatic fields, difficulties have been encountered in predicting the effects these fields have on the frost formation. Until recently, no satisfactory results, either qualitative or quantitative, have been available. In an effort to explain qualitatively some of the experimentally observed phenomenon, the fundamental thermodynamic expressions that describe the effect electrostatic fields have on the vapor–solid phase change processes occurring during frost formation, have been developed.

Theoretical Analysis

Frost formation through sublimation is a process of ice-crystal growth in the gaseous phase. When a surface at a temperature below the freezing temperature (0°C at atmospheric pressure) comes into contact with moist air having a dew-point temperature greater than the temperature of the surface, frost will form. Because the oversaturated water vapor is a metastable phase in which the Gibbs free energy is higher than that of an ice crystal in steady state, ice crystals can form (even under steady-state conditions). Assuming that the water vapor behaves as an ideal gas, the driving force of sublimation may be expressed as

$$f = RT \ln(P^*/P) \tag{1}$$

As a result of the oversaturated vapor pressure of the water

Received Oct. 10, 1994; revision received Jan. 27, 1995; accepted for publication Jan. 30, 1995.

*Graduate Research Assistant, Department of Mechanical Engineering.
†Tenneco Professor and Head, Department of Mechanical Engineering. Associate Fellow AIAA.